

Marquette University
e-Publications@Marquette

Chemistry Faculty Research and Publications

Chemistry, Department of

1-1-2013

Equivalence of the Ehrenfest Theorem and the Fluid-rotor Model for Mixed Quantum/Classical Theory of Collisional Energy Transfer

Alexander Semenov
Marquette University

Dmitri Babikov
Marquette University, dmitri.babikov@marquette.edu

Published version. *Journal of Chemical Physics*, Vol. 138 (2013): 164110. DOI. © 2013 American Institute of Physics. Used with permission.

Equivalence of the Ehrenfest theorem and the fluid-rotor model for mixed quantum/classical theory of collisional energy transfer

Alexander Semenov and Dmitri Babikov^{a)}

Department of Chemistry, Wehr Chemistry Building, Marquette University, Milwaukee, Wisconsin 53201-1881, USA

(Received 26 February 2013; accepted 27 March 2013; published online 23 April 2013)

The theory of two seemingly different quantum/classical approaches to collisional energy transfer and ro-vibrational energy flow is reviewed: a heuristic fluid-rotor method, introduced earlier to treat recombination reactions [M. Ivanov and D. Babikov, *J. Chem. Phys.* **134**, 144107 (2011)], and a more rigorous method based on the Ehrenfest theorem. It is shown analytically that for the case of a diatomic molecule + quencher these two methods are entirely equivalent. Notably, they both make use of the average moment of inertia computed as inverse of average of inverse of the distributed moment of inertia. Despite this equivalence, each of the two formulations has its own advantages, and is interesting on its own. Numerical results presented here illustrate energy and momentum conservation in the mixed quantum/classical approach and open opportunities for computationally affordable treatment of collisional energy transfer. © 2013 AIP Publishing LLC. [<http://dx.doi.org/10.1063/1.4801430>]

I. INTRODUCTION

Collisional energy transfer (CET)¹ encompasses a relatively broad spectrum of molecular phenomena where the energized *molecule* (typically small polyatomic molecule or a diatomic molecule) exchanges translational, rotational, and vibrational energy with a *quencher* (an atom, molecule, or even a surface). The result of such collision is usually a non-reactive inelastic scattering process, but dissociation of the molecule and/or the quencher may also occur. In some applications, the focus is on quenching of the low-lying internal states of the molecule (e.g., few quanta of ro-vibrational excitation^{2–8}) while in other processes, such as recombination reactions,^{9–13} the molecule is initially at energy above the dissociation threshold (scattering resonance). Several processes that are reverse to quenching, such as collisional excitation and the collision-induced dissociation, also fall into the category of the collisional energy transfer.

The relevant range of temperatures is very broad too. In recent years, the interest in collisional energy transfer at ultra-cold conditions has been high^{14–16} and in those cases the inelastic scattering calculations must be done using the full-fledged quantum mechanics.^{17,18} On the other hand, for the processes relevant to combustion,^{19,20} photochemistry,^{21,22} or hyper-thermal phenomena,^{23,24} when high energies are involved, the classical-trajectory picture is quite appropriate.^{25–29} In between those limits, the quantum mechanical calculations of collisional energy transfer become unaffordable computationally even for the smallest molecular systems (due to a large number of coupled channels and partial waves) while the classical trajectory calculations are not entirely justified and contain serious drawbacks (such as

vibrational zero-point energy leakage^{30,31}). Indeed, the vibrational frequencies are typically on order of one-to-few thousand wave numbers, so, the classical approximation for vibrational motion becomes truly valid only at very high temperatures. In polyatomic molecules, the vibrational spacing may be smaller but still, for the temperature range say $30 < T < 3000$ K (depending on system), there is no practical method of computing the collisional energy transfer. And this is exactly the temperature interval where majority of chemical processes occur.

The general idea to use a mixture of quantum and classical mechanics for description of collisional energy transfer is not new.^{32–34} However, it has never been developed to the level of predictive computational tool. The literature on this topic is surprisingly sparse. Some authors neglect rotational motion of the molecule,^{35–37} which is physically incorrect because the rotational energy transfer is usually a major pathway of the process. There are very few papers where rotational excitation of the molecule by the quencher was actually treated,^{33,34} but even there the molecule was assumed to have zero angular momentum prior to collision. Such an approach is able to give some insight into rotational excitation, but no information about rotational quenching. It is also obvious that collision of a rotationless molecule with quencher would lead to overestimated rotational excitation (even statistically) since all the available rotational states are unpopulated before collision. It is desirable to specify adequate thermal initial conditions for rotation.

Clearly, there are ample opportunities for development of new theories of collisional energy transfer. Recently, the mixed quantum/classical theory (MQCT) for CET and ro-vibrational energy flow (RVEF) was proposed^{11,12} and applied to treat a very complicated problem – recombination reaction that forms ozone.^{13,38} In this approach, the time-dependent quantum mechanics (wave packet method) is

^{a)} Author to whom correspondence should be addressed. Electronic mail: dmitri.babikov@mu.edu

used to treat vibrational motion of the energized molecule, while its rotational motion and scattering of the quencher are treated with classical trajectories. The rotation-vibration interaction is included in an adiabatic manner, within the *fluid-rotor* model. Energy is exchanged between translational, rotational, and vibrational degrees of freedom, while the total energy of the system is conserved. This method allows capturing major quantum effects associated with vibrational motion of the molecule (i.e., zero-point energy, quantization of states, tunneling, scattering resonances) while the advantage is taken of the quasi-classical regime usually valid for rotational and translational degrees of freedom. This mixed quantum/classical approach is expected to be accurate in the intermediate temperature range $30 < T < 3000$ K and computationally affordable for small polyatomic molecules.

In the present paper, we review this approach and demonstrate that it is, in fact, equivalent to the Ehrenfest theorem treatment of the process. Detailed theory is presented for the simplest energy-transfer process – collision of a diatomic molecule with a quencher. The paper is organized as follows. In Sec. II, we outline major components of MQCT for CET and RVEF. In Sec. III, we review the Ehrenfest theorem treatment of the diatom + atom collision and show analytically that it is equivalent to the fluid-rotor model. Some illustrative numerical results are presented in Sec. IV. Conclusions and possible applications of this theory are given in Sec. V.

II. THEORETICAL FRAMEWORK

A set of internal coordinates of the molecule is denoted \mathbf{R}_Q , where subscript “Q” is used to stress that these degrees of freedom are treated quantum mechanically. The vibrational wave function $\Psi(\mathbf{R}_Q)$ is expressed in these coordinates and is represented by a suitable grid of points. For example, in the case of a diatomic molecule \mathbf{R}_Q represents only one degree of freedom – the bond length R . In the case of a triatomic molecule $\mathbf{R}_Q = \{R_1, R_2, \theta\}$ defines two bond lengths and bending angle, so, the grid is three-dimensional. The time-dependent Schrödinger equation for vibrational motion (neglecting rotation)

$$i \frac{\partial}{\partial t} \Psi(\mathbf{R}_Q, t) = \hat{H}(t) \Psi(\mathbf{R}_Q, t), \quad (1)$$

$$\hat{H}(t) = \hat{T} + V(\mathbf{R}_Q; \mathbf{R}_C(t)), \quad (2)$$

is propagated using the wave packet method.³⁹ Note that Hamiltonian $\hat{H}(t)$ is time dependent and this dependence comes from the potential energy term. If the quencher is at infinity, this term represents potential energy surface of the molecule $V(\mathbf{R}_Q)$. As the quencher approaches and scatters off the molecule, the potential energy surface is continuously modified due to the quencher-molecule interaction, which is formally written as $V(\mathbf{R}_Q; \mathbf{R}_C(t))$ dependence. Here, \mathbf{R}_C denotes the external (scattering) degrees of freedom, treated classically. If rotational motion is neglected, those are just the center-of-mass positions for molecule and quencher – six Cartesian coordinates in the laboratory-fixed reference frame, $\mathbf{R}_C = \{\mathbf{q}_{\text{mol}}, \mathbf{q}_{\text{que}}\}$. So, the time-dependence of $\mathbf{R}_C(t)$

is governed by the classical trajectory of motion, which introduces time-dependence into the Hamiltonian $\hat{H}(t)$. In this way, scattering of the quencher affects vibrational motion of the molecule and classical part of the system affects its quantum part.

For the translational (scattering) degrees of freedom, the classical equations of motion are simply

$$\dot{\mathbf{q}} = \mathbf{p}/m, \quad (3)$$

$$\dot{\mathbf{p}} = -\nabla \tilde{V}, \quad (4)$$

where subscripts were omitted for transparency. The moiety \tilde{V} is the mean-field potential, which represents average of the potential energy of the system over the vibrational wave function of the molecule (quantum expectation value)

$$\tilde{V}(\mathbf{R}_C) = \langle \Psi(\mathbf{R}_Q) | V(\mathbf{R}_Q, \mathbf{R}_C) | \Psi(\mathbf{R}_Q) \rangle, \quad (5)$$

where integration is over \mathbf{R}_Q . Thus, gradients of the mean-field potential with respect to classical variables $\mathbf{R}_C = \{\mathbf{q}_{\text{mol}}, \mathbf{q}_{\text{que}}\}$ drive the scattering process. Note also that \tilde{V} reflects the internal vibrational state of the molecule, through average over the vibrational wave function $\Psi(\mathbf{R}_Q)$. In this way, the vibrational degrees of freedom affect the dynamics of scattering, and the state of the quantum part of the system affects motion of its classical part.

A. The fluid-rotor model

If the rotational motion of molecule is included and is treated classically, the set of classical degrees of freedom should be expanded to include Euler angles⁴⁰ used to define orientation of molecule in space: $\mathbf{R}_C = \{\mathbf{q}_{\text{mol}}, \mathbf{q}_{\text{que}}, \alpha, \beta, \gamma\}$. The effect of rotational motion on vibration is taken into account adiabatically,^{41–46} by introducing the centrifugal potential term V_{rot} into the Hamiltonian operator

$$\hat{H}(t) = \hat{T}_{J=0} + V(\mathbf{R}_Q; \mathbf{R}_C(t)) + V_{\text{rot}}(\mathbf{R}_Q; \mathbf{R}_C(t)). \quad (6)$$

This term represents rotational energy of the molecule and is a continuous smooth function of its shape (i.e., of the internal coordinates \mathbf{R}_Q). Also, V_{rot} is a function of time, since rotational energy changes along the trajectory $\mathbf{R}_C(t)$. At every moment of time and for every point \mathbf{R}_Q of the grid, we compute this potential numerically as

$$V_{\text{rot}}(\mathbf{R}_Q) = \frac{1}{2} (\mathbf{J}, \mathbf{I}^{-1}(\mathbf{R}_Q) \mathbf{J}), \quad (7)$$

where $\mathbf{I}(\mathbf{R}_Q)$ is the tensor of inertia on the grid and $\mathbf{J}(t)$ is the instantaneous vector of angular momentum of the molecule, both expressed in the laboratory reference frame. Note that this adiabatic rotation approximation is expected to work better than any other method of angular momentum decoupling, simply because tensor of inertia of the molecule is not fixed at a single chosen molecular configuration (e.g., equilibrium position), but changes smoothly as molecular shape is distorted by vibration. This feature is important for treatment of the large-amplitude vibrational motion (e.g., highly excited vibrations or even dissociation).

Equation (7) is also used to define the average tensor of inertia of the classical rotor, $\tilde{\mathbf{I}}$, that corresponds to vibrational

wave function $\Psi(\mathbf{R}_Q)$. For this, we require that quantum expectation value of rotational energy,

$$\tilde{E}_{\text{rot}}^Q = \langle \Psi(\mathbf{R}_Q) | V_{\text{rot}}(\mathbf{R}_Q) | \Psi(\mathbf{R}_Q) \rangle, \quad (8)$$

coincides with energy of the average classical rotor,

$$E_{\text{rot}}^C = \frac{1}{2}(\mathbf{J}, \tilde{\mathbf{I}}^{-1} \mathbf{J}), \quad (9)$$

at every moment of time. From $\tilde{E}_{\text{rot}}^Q = E_{\text{rot}}^C$, one obtains¹¹

$$\tilde{\mathbf{I}} = \langle \Psi(\mathbf{R}_Q) | \mathbf{I}^{-1}(\mathbf{R}_Q) | \Psi(\mathbf{R}_Q) \rangle^{-1}, \quad (10)$$

which guarantees conservation of total ro-vibrational energy and describes how evolution of vibrational wave function (treated with quantum mechanics) affects the tensor of inertia of the classical rotor.

Thus, vibrational and rotational degrees of freedom are treated explicitly and self-consistently. The rigid-rotor assumption of any sort is avoided and we deal with *fluid rotor*, whose tensor inertia $\tilde{\mathbf{I}}(t)$ is affected by vibration and is time-dependent. Equations for rotation of such fluid rotor are obtained as follows. Start with $\mathbf{J} = \tilde{\mathbf{I}}\boldsymbol{\omega}$ and, assuming that each of these quantities is time dependent, differentiate this expression (by parts) with respect to time: $d\mathbf{J}/dt = \dot{\tilde{\mathbf{I}}}\boldsymbol{\omega} + \tilde{\mathbf{I}}\dot{\boldsymbol{\omega}}$. Introduce average torque as

$$\tilde{\boldsymbol{\tau}} = d\mathbf{J}/dt. \quad (11)$$

Express angular velocities $\boldsymbol{\omega}(t)$ and accelerations $\dot{\boldsymbol{\omega}}(t)$ through Euler angles

$$\boldsymbol{\omega} = \mathbf{G} \begin{pmatrix} \dot{\alpha} \\ \dot{\beta} \\ \dot{\gamma} \end{pmatrix}, \quad (12)$$

where, for convenience, we defined

$$\mathbf{G} = \begin{pmatrix} 0 & \cos \alpha & \sin \beta \sin \alpha \\ 0 & \sin \alpha & -\sin \beta \cos \alpha \\ 1 & 0 & \cos \beta \end{pmatrix}. \quad (13)$$

Further manipulations¹¹ lead to the following final system of second-order differential equations for rotation of the fluid rotor

$$\begin{pmatrix} \ddot{\alpha} \\ \ddot{\beta} \\ \ddot{\gamma} \end{pmatrix} = \mathbf{G}^{-1} \left[\tilde{\mathbf{I}}^{-1} \left[\tilde{\boldsymbol{\tau}} - \dot{\tilde{\mathbf{I}}}\mathbf{G} \begin{pmatrix} \dot{\alpha} \\ \dot{\beta} \\ \dot{\gamma} \end{pmatrix} \right] - \dot{\mathbf{G}} \begin{pmatrix} \dot{\alpha} \\ \dot{\beta} \\ \dot{\gamma} \end{pmatrix} \right]. \quad (14)$$

Time-derivative of the mean tensor, $\dot{\tilde{\mathbf{I}}}$ in Eq. (14), can be computed by differentiating over time the definition of $\tilde{\mathbf{I}}$,

Eq. (10)

$$\dot{\tilde{\mathbf{I}}} = \tilde{\mathbf{I}}\mathbf{A}\tilde{\mathbf{I}}, \quad (15)$$

where

$$\mathbf{A} = \langle \Psi | \mathbf{I}^{-1} \left(\frac{d\mathbf{I}}{dt} \right) \mathbf{I}^{-1} | \Psi \rangle - 2\text{Re} \langle \Psi | \mathbf{I}^{-1} \left| \frac{d}{dt} \Psi \right\rangle. \quad (16)$$

Note that in the rigid-rotor case, when vibrational wave function of the molecule does not evolve, $d\Psi/dt = 0$ and the second term in Eq. (17) vanishes.

The mean torque $\tilde{\boldsymbol{\tau}}$ in Eq. (14) is computed as average over the vibrational wave function

$$\tilde{\boldsymbol{\tau}} = -\langle \Psi(\mathbf{R}_Q) | \sum_i \mathbf{r}_i \times \nabla V | \Psi(\mathbf{R}_Q) \rangle, \quad (17)$$

where $\mathbf{r}_i \times \nabla V$ represents torque of the quencher on each atom in the molecule, $\mathbf{r}_i = \{x_i, y_i, z_i\}$ is radius vector of i th atom relative to molecular center or mass, the gradient ∇V is computed with respect to Cartesian position of each atom. Summation in Eq. (17) is over all atoms in the molecule (e.g., three for a triatomic molecule).

In the way, formulated above this theory can be applied to small polyatomic molecules. The fluid rotor treatment of rotation is computationally inexpensive. The most demanding part is propagation of the time-dependent Schrodinger equation for vibration, Eq. (1) with Hamiltonian (6). As size of the molecule increases ($3N - 6$ vibrational degrees of freedom for N -atomic molecule), integrating the quantum expectation values in Eqs. (5), (10), (15), and (17) also becomes costly. The case of triatomic molecule was discussed in detail in Ref. 11. Diatomic molecule is a special case, discussed in Sec. II B below.

B. Diatomic molecule + quencher

Relative to molecular center of mass, the coordinates of two atoms ($i = 1, 2$) are given by

$$x_i = R \frac{m_i}{m_1 + m_2} \cos \alpha \sin \gamma, \quad (18a)$$

$$y_i = R \frac{m_i}{m_1 + m_2} \sin \alpha \sin \gamma, \quad (18b)$$

$$z_i = R \frac{m_i}{m_1 + m_2} \cos \gamma. \quad (18c)$$

Substitution of Eqs. (18a)–(18c) into standard expression for the tensor of inertia,

$$\mathbf{I} = \begin{pmatrix} \sum m_i (y_i^2 + z_i^2) & -\sum m_i x_i y_i & -\sum m_i z_i x_i \\ -\sum m_i x_i y_i & \sum m_i (x_i^2 + z_i^2) & -\sum m_i z_i y_i \\ -\sum m_i z_i x_i & -\sum m_i z_i y_i & \sum m_i (x_i^2 + y_i^2) \end{pmatrix}, \quad (19)$$

leads to

$$\mathbf{I} = I \mathbf{M}, \quad (20)$$

where matrix \mathbf{M} is defined as

$$\mathbf{M} = \begin{pmatrix} \sin^2 \gamma \sin^2 \alpha + \cos^2 \gamma & -\sin^2 \gamma \sin \alpha \cos \alpha & -\sin \gamma \cos \gamma \cos \alpha \\ -\sin^2 \gamma \sin \alpha \cos \alpha & \sin^2 \gamma \cos^2 \alpha + \cos^2 \gamma & -\sin \gamma \cos \gamma \sin \alpha \\ -\sin \gamma \cos \gamma \cos \alpha & -\sin \gamma \cos \gamma \sin \alpha & \sin^2 \gamma \end{pmatrix}, \quad (21)$$

and a scalar $I = \mu R^2$ gives the moment of inertia of the diatomic, expressed through its reduced mass $\mu = m_1 m_2 / (m_1 + m_2)$. The matrix \mathbf{M} is singular. Thus, the tensor of inertia \mathbf{I} cannot be inverted, and all equations above that contain \mathbf{I}^{-1} should be rewritten in the way suitable for the case of diatomic molecule. Those are Eqs. (7), (9), (10), and (14).

For rotational potential and rotational energy of the diatomic fluid rotor, instead of Eqs. (7) and (9), we can write

$$V_{\text{rot}}(\mathbf{R}_Q) = \frac{\mathbf{J}^2}{2\mu R^2} = \frac{\mathbf{J}^2}{2I(R)}, \quad (7')$$

$$E_{\text{rot}}^C = \frac{\mathbf{J}^2}{2\tilde{I}}. \quad (9')$$

Substituting Eq. (7') into Eq. (8) and equating the result to Eq. (9'), leads to the following expression for the mean moment of inertia of the diatomic fluid rotor:

$$\tilde{I} = \langle \Psi(R) | \frac{1}{\mu R^2} | \Psi(R) \rangle^{-1}. \quad (10')$$

Here, the vibrational wave function $\Psi(R)$ is one-dimensional. This scalar expression replaces the vector expression of Eq. (10). From Eq. (20), it also follows that $\tilde{\mathbf{I}} = \tilde{I} \mathbf{M}$.

Positioning the diatomic molecule in space requires only two Euler angles, α and γ , that correspond to spherical polar coordinates. The value of β is constant, arbitrary, and can be set to $\beta = \pi/2$, for convenience. Thus, Eqs. (12) and (13) transform into

$$\boldsymbol{\omega} = \mathbf{G} \begin{pmatrix} \dot{\alpha} \\ 0 \\ \dot{\gamma} \end{pmatrix} \quad (12')$$

and

$$\mathbf{G} = \begin{pmatrix} 0 & \cos \alpha & \sin \alpha \\ 0 & \sin \alpha & -\cos \alpha \\ 1 & 0 & 0 \end{pmatrix}. \quad (13')$$

Equation (14) can be formally rewritten as

$$\tilde{\mathbf{I}} \mathbf{G} \begin{pmatrix} \ddot{\alpha} \\ 0 \\ \ddot{\gamma} \end{pmatrix} = \tilde{\boldsymbol{\tau}} - [\tilde{\mathbf{I}} \mathbf{G} + \dot{\tilde{\mathbf{I}}} \mathbf{G}] \begin{pmatrix} \dot{\alpha} \\ 0 \\ \dot{\gamma} \end{pmatrix}. \quad (14')$$

Note that although many elements of these 3×3 matrixes are zero, it is impossible to express Eq. (14') through 2×2 matrixes, simply because the torque $\tilde{\boldsymbol{\tau}}$, occurring during the molecule-quencher collision, is represented by a 3×3 matrix and, in general, none of its elements is zero. This property

is also related to evolution of the angular momentum vector, due to torque supplied by the quencher, according to Eq. (11). Of course, in the absence of external torque, rotation of a diatomic is essentially two-dimensional and could be described by 2×2 matrixes in the appropriate reference frame.

III. THE EHRENFEST THEOREM

The theorem of Ehrenfest provides a link between the expectation values of quantum operators $\langle \hat{\mathbf{q}} \rangle$ and $\langle \hat{\mathbf{p}} \rangle$, and their classical counterparts – generalized positions and momenta, \mathbf{q} and \mathbf{p} . This theorem is employed in order to obtain classical equations of motion for the system which contains quantum and classical degrees of freedom. The main idea is to start with “mixed” Hamiltonian of the system, which already includes classical variables and quantum operators, and derive classical Hamiltonian by averaging quantum part over the wave function. From such classical Hamiltonian, one can derive equations of motion for classical variables. The Ehrenfest approach involves assumption that each classical trajectory is independent from other individual trajectories.⁴⁷ Generally, the Ehrenfest approach is valid if state-to-state transitions in the quantum part of the system do not modify drastically the dynamics of its classical part.⁴⁸ This is the case if transition probabilities are relatively small, or if wave functions of different quantum states lead to similar expectation values.

A. General theory for diatomic + atom

Using notations of Sec. II A, the total Hamiltonian operator for the system of diatomic molecule + atom can be written as

$$\hat{H} = -\frac{\hbar^2}{2\mu R^2} \frac{\partial}{\partial R} R^2 \frac{\partial}{\partial R} + \hat{T}_{\text{rot}} + \frac{\hat{\mathbf{p}}_{\text{mol}}^2}{2m_{\text{mol}}} + \frac{\hat{\mathbf{p}}_{\text{que}}^2}{2m_{\text{que}}} + V(R, \alpha, \gamma, \mathbf{q}_{\text{mol}}, \mathbf{q}_{\text{que}}). \quad (22)$$

Replacing the radial wave function $\Phi(R)$ by new wave function $\Psi(R) = \Phi(R)/R$ permits to simplify the kinetic energy operator and calculate the volume element as $|\Psi(R)|^2 dR = |\Phi(R)|^2 R^2 dR$. Expressing the rotational kinetic energy operator in spherical polar coordinates in the Laplace-Beltrami form,⁴⁹ using $\hat{p}_\alpha = -i\hbar \partial / \partial \alpha$ and $\hat{p}_\gamma = -i\hbar \partial / \partial \gamma$, leads to the following expression for the Hamiltonian operator:

$$\hat{H} = -\frac{\hbar^2}{2\mu} \frac{\partial^2}{\partial R^2} + \frac{\hat{p}_\gamma \sin \gamma \hat{p}_\gamma}{2\mu R^2 \sin \gamma} + \frac{\hat{p}_\alpha^2}{2\mu R^2 \sin^2 \gamma} + \frac{\hat{\mathbf{p}}_{\text{mol}}^2}{2m_{\text{mol}}} + \frac{\hat{\mathbf{p}}_{\text{que}}^2}{2m_{\text{que}}} + V(R, \alpha, \gamma, \mathbf{q}_{\text{mol}}, \mathbf{q}_{\text{que}}). \quad (23)$$

Next step is to separate all degrees of freedom in the system onto quantum (vibration) and classical (rotation and translation). Thus, $\mathbf{R}_Q = \{R\}$ and $\mathbf{R}_C = \{\mathbf{q}_{\text{mol}}, \mathbf{q}_{\text{que}}, \alpha, \gamma\}$. For classical degrees of freedom, we replace quantum operators \hat{p}_α , \hat{p}_γ , $\hat{\mathbf{p}}_{\text{mol}}$, and $\hat{\mathbf{p}}_{\text{que}}$ by their classical analogues, and split Hamiltonian onto two parts. The quantum Hamiltonian is

$$\hat{H}_Q = -\frac{\hbar^2}{2\mu} \frac{\partial^2}{\partial R^2} + \frac{p_\gamma^2}{2\mu R^2} + \frac{p_\alpha^2}{2\mu R^2 \sin^2 \gamma} + V(\mathbf{R}_Q; \mathbf{R}_C(t)). \quad (24)$$

The classical Hamiltonian is obtained as expectation value

$$\begin{aligned} H_C &= \langle \Psi(R) | \hat{H} | \Psi(R) \rangle \\ &= \frac{\mathbf{p}_{\text{mol}}^2}{2m_{\text{mol}}} + \frac{\mathbf{p}_{\text{que}}^2}{2m_{\text{que}}} + \langle \Psi(R) | \hat{H}_Q | \Psi(R) \rangle \\ &= \frac{\mathbf{p}_{\text{mol}}^2}{2m_{\text{mol}}} + \frac{\mathbf{p}_{\text{que}}^2}{2m_{\text{que}}} + \left(\frac{p_\gamma^2}{2\mu} + \frac{p_\alpha^2}{2\mu \sin^2 \gamma} \right) \\ &\quad \times \langle \Psi(R) | \frac{1}{R^2} | \Psi(R) \rangle + \tilde{T}_Q + \tilde{V}(\mathbf{R}_C). \end{aligned} \quad (25)$$

Note that this expression can be conveniently rewritten by introducing \tilde{I} defined in Eq. (10'). Indeed,

$$H_C = \frac{\mathbf{p}_{\text{mol}}^2}{2m_{\text{mol}}} + \frac{\mathbf{p}_{\text{que}}^2}{2m_{\text{que}}} + \frac{p_\gamma^2}{2\tilde{I}} + \frac{p_\alpha^2}{2\tilde{I} \sin^2 \gamma} + \tilde{T}_Q + \tilde{V}(\mathbf{R}_C). \quad (26)$$

Here, $\tilde{V}(\mathbf{R}_C)$ is the mean field potential, just as one in Eq. (5). Expectation value of quantum kinetic energy in Eq. (26),

$$\tilde{T}_Q = -\frac{\hbar^2}{2\mu} \langle \Psi(R) | \frac{\partial^2}{\partial R^2} | \Psi(R) \rangle, \quad (27)$$

is not a function of any classical coordinates. It is only a function of time.

From classical Hamiltonian of Eq. (26), the equations of motions can be obtained in a standard way: $\dot{\mathbf{q}} = \partial H_C / \partial \mathbf{p}$ and $\dot{\mathbf{p}} = -\partial H_C / \partial \mathbf{q}$. For translational degrees of freedom \mathbf{q}_{mol} and \mathbf{q}_{que} , one obtains equations exactly equivalent to Eqs. (3)–(5). For rotational degrees of freedom α and γ , this gives

$$\dot{\alpha} = \frac{p_\alpha}{\tilde{I} \sin^2 \gamma}, \quad (28a)$$

$$\dot{\gamma} = \frac{p_\gamma}{\tilde{I}}, \quad (28b)$$

$$\dot{p}_\alpha = -\frac{\partial \tilde{V}}{\partial \alpha}, \quad (28c)$$

$$\dot{p}_\gamma = -\frac{\partial \tilde{V}}{\partial \gamma} + \frac{p_\alpha^2 \cos \gamma}{2\tilde{I} \sin^3 \gamma}. \quad (28d)$$

Similar equations for rigid rotor are well known,⁴⁹ but here the emphasis is on definition of the average moment of inertia \tilde{I} given by Eq. (10').

One could erroneously think that \tilde{I} should be computed using the average value of vibrational coordinate $\tilde{R} = \langle \Psi(R) | R | \Psi(R) \rangle$, but the theory presented above shows that $\tilde{I} \neq \mu \tilde{R}^2$. Another possibility that may seem quite appropriate (but is also incorrect) is to compute \tilde{I} as the average value of $I(R)$. However, one should realize that \tilde{I}

$\neq \langle \Psi(R) | I(R) | \Psi(R) \rangle$. Instead, \tilde{I} must be computed as inverse of average of the inverse: $\tilde{I} = \langle \Psi(R) | I^{-1}(R) | \Psi(R) \rangle^{-1}$. This expression is not trivial and, to our best knowledge, is not well known, even for a diatomic molecule. It originates from averaging the rotational energy, rather than vibrational coordinate or the moment of inertia.

What are the consequences of using an incorrect expression to compute \tilde{I} ? For a *compact* wave packet $\Psi(R)$, like the ground vibrational state wave function, the differences between $\langle \Psi(R) | R | \Psi(R) \rangle^2$, $\langle \Psi(R) | R^2 | \Psi(R) \rangle$, and $\langle \Psi(R) | R^{-2} | \Psi(R) \rangle^{-1}$ can be small. However, for the large-amplitude vibrational motion characterized by a *broad* wave function the effect can be sizable. Examples include such processes as collision-induced dissociation, dynamics of the van der Waals states, or large-amplitude bending motion of a floppy molecule. Also, from the fundamental theory perspective, the total energy of the mixed quantum/classical system is conserved only if the correct expression $\tilde{I} = \langle \Psi(R) | I^{-1}(R) | \Psi(R) \rangle^{-1}$ is used for the classical rotor (see Sec. IV).

B. Equivalence of the two methods

It is interesting that the expression $\tilde{I} = \langle \Psi(R) | I^{-1}(R) | \Psi(R) \rangle^{-1}$ appears in both the fluid-rotor equations and in the Ehrenfest theorem treatment. In the first case, it emerges from the requirement that expectation value of quantum rotational energy \tilde{E}_{rot}^Q equals to classical energy of the fluid rotor E_{rot}^C , at every moment of time, which guaranteed conservation of total energy. In the second case, it comes from averaging the quantum Hamiltonian, with the purpose of obtaining its classical counterpart. These sources seem to be related.

There are, however, two pronounced differences between the two methods. First, the rigid rotor equation (14) include $\dot{\tilde{I}}$ and require the knowledge of $d\Psi/dt$ in Eq. (16), while there is no time-derivative of wave function involved in Eqs. (28a)–(28d). Second, expression (17) for the mean torque includes summation over all atoms in a molecule, while there is nothing like that in Eqs. (28a)–(28d). So, the question can be raised: Are those two methods entirely equivalent, or the expression for \tilde{I} is the only thing they have in common?

On one side, the Hamiltonian equations (28a)–(28d) can be combined into the second-order equations, by differentiating over time both sides of Eqs. (28a) and (28b), and substituting Eqs. (28c) and (28d) as appropriate

$$(\tilde{I}\ddot{\alpha} + \dot{\tilde{I}}\dot{\alpha}) \sin^2 \gamma = -2\tilde{I}\dot{\alpha}\dot{\gamma} \cos \gamma \sin \gamma - \frac{\partial \tilde{V}}{\partial \alpha}, \quad (29)$$

$$\tilde{I}\ddot{\gamma} + \dot{\tilde{I}}\dot{\gamma} = 2\tilde{I}\dot{\alpha}^2 \cos \gamma \sin \gamma - \frac{\partial \tilde{V}}{\partial \gamma}. \quad (30)$$

On the other side, we can work with the fluid rotor equations and substitute (13'), (20), and (21) into (14'). This leads to the matrix equation given in Appendix A. Let us look at its z -component first, Eq. (A3)

$$\tilde{I}\ddot{\alpha} \sin^2 \gamma = \tilde{\tau}_z - \dot{\tilde{I}}\dot{\alpha} \sin^2 \gamma - 2\tilde{I}\dot{\gamma}\dot{\alpha} \sin \gamma \cos \gamma. \quad (31)$$

Interestingly, this equation becomes equivalent to Eq. (29), if we can show that

$$\tilde{\tau}_z = -\frac{\partial \tilde{V}}{\partial \alpha}. \quad (32)$$

This is done in Eqs. (B1) and (B2) of Appendix B, which proves that z -component of Eq. (14') is equivalent to Eqs. (28a) and (28c).

In a similar manner, we can combine x - and y -components of Eq. (14'), given as expressions (A1) and (A2) in Appendix A, into the expression similar to Eq. (30). Namely, multiplying (A1) by $\sin \alpha$ and subtracting (A2) multiplied by $\cos \alpha$, we obtain

$$\begin{aligned} & \tilde{I}(\dot{\gamma} \sin \alpha - \ddot{\alpha} \sin \gamma \cos \gamma \cos \alpha) \sin \alpha \\ & - \tilde{I}(-\dot{\gamma} \cos \alpha - \ddot{\alpha} \sin \gamma \cos \gamma \sin \alpha) \cos \alpha \\ & = [\tilde{\tau}_x - \dot{\tilde{I}}(\dot{\gamma} \sin \alpha - \ddot{\alpha} \sin \gamma \cos \gamma \cos \alpha) \\ & \quad - \tilde{I} \dot{\alpha}^2 \sin \gamma \cos \gamma \sin \alpha] \sin \alpha \\ & - [\tilde{\tau}_y - \dot{\tilde{I}}(-\dot{\gamma} \cos \alpha - \ddot{\alpha} \sin \gamma \cos \gamma \sin \alpha) \\ & \quad + \tilde{I} \dot{\alpha}^2 \sin \gamma \cos \gamma \cos \alpha] \cos \alpha. \end{aligned} \quad (33)$$

In this expression, several terms cancel and it becomes, indeed, equivalent to Eq. (30), if we can prove that

$$\tilde{\tau}_x \sin \alpha - \tilde{\tau}_y \cos \alpha = -\frac{\partial \tilde{V}}{\partial \gamma}. \quad (34)$$

This finalizes our prove that Eqs. (28a)–(28d) are equivalent to Eq. (14'). Here, we showed that not only the definition of \tilde{I} is the same in both methods, but also that the heuristic “fluid-rotor” approach (introduced *ad hoc* in Ref. 11 and used to treat the collisional energy transfer in recombination reaction^{13,38}) is, in fact, entirely equivalent to the Ehrenfest theorem treatment of this process.

IV. NUMERICAL RESULTS

In order to gain further insight into the mixed quantum/classical approach to collisional energy transfer, we carried out numerical simulations of CO ($v = 1$) quenching by He impact, using Eqs. (28a)–(28d) and (10'). Potential energy surface from Ref. 7 was employed. Calculations of converged cross sections for this process in a broad range of temperatures, $30 < T < 3000$ K, will be reported in Ref. 50. Here, we focus on fundamentally important issues of ro-vibrational energy transfer, total energy conservation, and time evolution of $\tilde{I}(t)$. We used the Runge-Kutta method of 4th order⁵¹ for classical degrees of freedom and the Lanczos propagator³⁹ for quantum degrees of freedom.

We will analyze one representative trajectory that starts with CO ($v = 1$) in a highly excited rotational state $J = 45$. The He atom collides with the molecule with relatively small impact parameter $b = 2.58 a_0$ and the center-of-mass translational energy $E_{\text{col}} = 4000 \text{ cm}^{-1}$. The collision geometry is rather arbitrary, neither planar nor perpendicular.

Figure 1 shows evolution of $\tilde{I}(t)$. Before collision the vibrational wave packet corresponds to an eigenstate $v = 1$ and we see that the value of \tilde{I} remains constant. During the

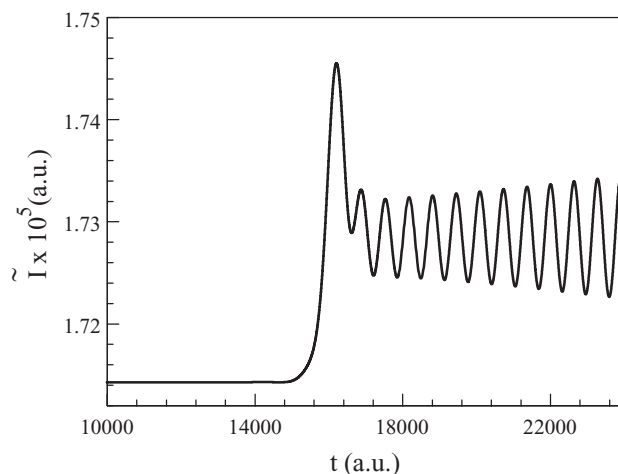


FIG. 1. Time evolution of the average moment of inertia of CO molecule $\tilde{I}(t)$ along the example trajectory discussed in the text. The post-collisional dynamics is clearly seen.

collision it starts changing, and oscillates quite dramatically at the post-collisional state. Clearly, oscillations of $\tilde{I}(t)$ correspond to the motion of vibrational wave packet which, in this case, includes appreciable populations of eigenstates up to $v = 3$. This is illustrated by Fig. 2, where we plotted populations of vibrational states along the trajectory, determined by projecting the vibrational wave packet onto the instantaneous vibrational basis, i.e., the vibrational eigenstates computed at each moment of time using the instantaneous value of $J(t) = \sqrt{p_\gamma^2 + p_\alpha^2 / \sin^2 \gamma}$. Vibrational state-to-state transitions are clearly seen for $v = 0, 1, 2$, and 3. Note that for this trajectory the angular momentum transfer is quite significant, $\Delta J \approx -19$, so that the initial and the final vibrational spectra are very different. However, despite dramatic vibrational motion and oscillations of $\tilde{I}(t)$ during the post-collisional dynamics, the value of J remains constant (within accuracy of the numerical method, very high here, $\delta J \approx 10^{-6}$). This demonstrates conservation of the angular momentum.

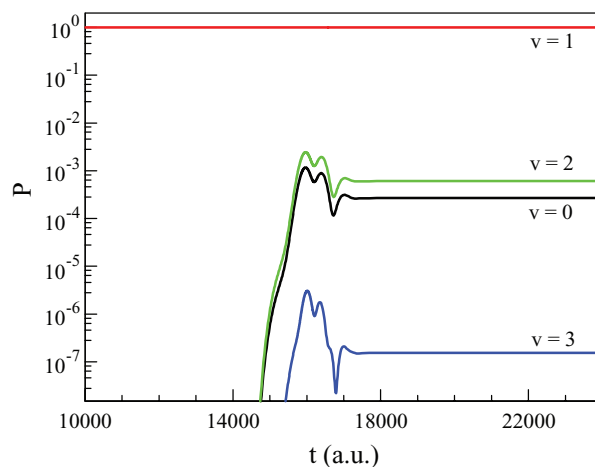


FIG. 2. Evolution of vibrational state populations in CO during its collision with He atom, as they follow the example trajectory discussed in the text. Vibrational state-to-state transitions occur during the relatively short time of collision.

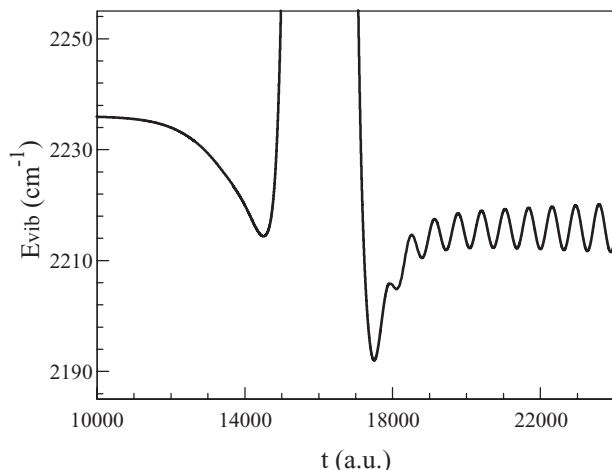


FIG. 3. Evolution of average vibrational energy of CO (quantum expectation value) during its collision with He atom, as they follow the example trajectory discussed in the text. The post-collisional dynamics is seen.

Figure 3 shows expectation value of quantum vibrational energy $\tilde{E}_{\text{vib}} = \langle \Psi(R) | \hat{T} + V(R) | \Psi(R) \rangle$ computed along the trajectory and Fig. 4 shows evolution of classical rotational energy $\tilde{E}_{\text{rot}} = J^2/2I$. Clearly, the post-collisional stage of the process exhibits very pronounced and ongoing ro-vibrational energy exchange, with amplitude close to 10 cm^{-1} . Indeed, comparing Figs. 3 and 4, one can see that oscillations of \tilde{E}_{vib} and \tilde{E}_{rot} are out of phase (shifted by π). The total energy is conserved with very high precision, $\delta E \approx 10^{-2} \text{ cm}^{-1}$, defined only by accuracy of the numerical integration method. Overall, in this collision the molecule lost about $\Delta E_{\text{tot}} = 2580 \text{ cm}^{-1}$. On average, $\Delta \tilde{E}_{\text{rot}} \approx 2560 \text{ cm}^{-1}$ and $\Delta \tilde{E}_{\text{vib}} \approx 20 \text{ cm}^{-1}$.

Careful analysis of the long time behavior during the post-collisional stage shows two characteristic frequencies of oscillations in $\tilde{I}(t)$, \tilde{E}_{vib} , and \tilde{E}_{rot} . One (higher) frequency is very obvious from Figs. 1, 3, and 4. It corresponds to vibrational motion of the molecule. The second (lower) frequency corresponds to vibrational inharmonicity. It manifests as slight modulation of the vibrational oscillation amplitude

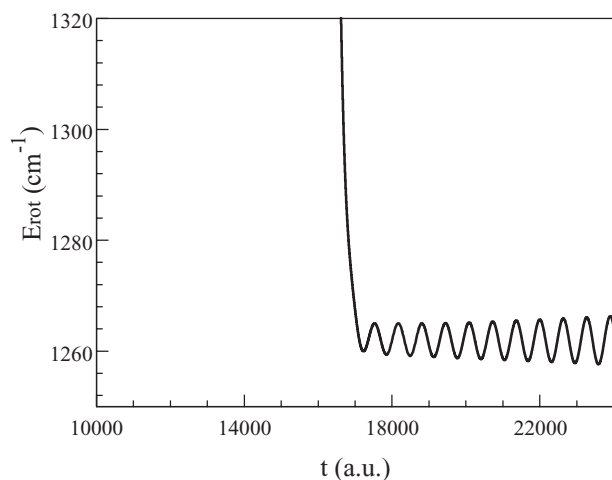


FIG. 4. Evolution of classical rotational energy of CO during its collision with He atom, as colliding partners follow the example trajectory discussed in the text. The post-collisional dynamics is seen.

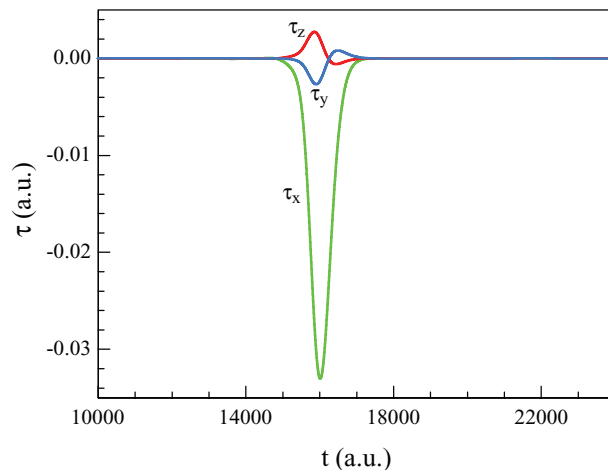


FIG. 5. Evolution of three Cartesian components of torque $\tilde{\tau}$, as CO collides with He atom, following the example trajectory discussed in the text.

in $\tilde{I}(t)$, \tilde{E}_{vib} , and \tilde{E}_{rot} . Although not very clear but, still, this effect can be seen in Fig. 1, which captures quarter-period of this low frequency dynamics.

Figure 5 shows evolution of three components of the mean torque $\tilde{\tau}$ during the moment of collision. All of them contribute to rotational de-excitation of the molecule and vanish when the collision is over. This is expected, since the geometry of collision is pseudo-arbitrary and the process is treated in the three-dimensional space, even though the instantaneous rotation of the diatomic molecule at each moment of time is essentially two-dimensional.

Coming back to the question of energy conservation, we repeated calculations for the same trajectory two more times: one using $\mu \langle \Psi(R) | R | \Psi(R) \rangle^2$ and second using $\mu \langle \Psi(R) | R^2 | \Psi(R) \rangle$ for \tilde{I} , instead of the correct $\tilde{I} = \mu \langle \Psi(R) | R^{-2} | \Psi(R) \rangle^{-1}$ of Eq. (10'). In each test-case, we computed the change of total energy in the system, δE . Results are presented in Fig. 6 and we see that the total energy is conserved only in the original correct case (green line). In two test-cases, some energy was lost: $\delta E \approx 6.0 \text{ cm}^{-1}$ and

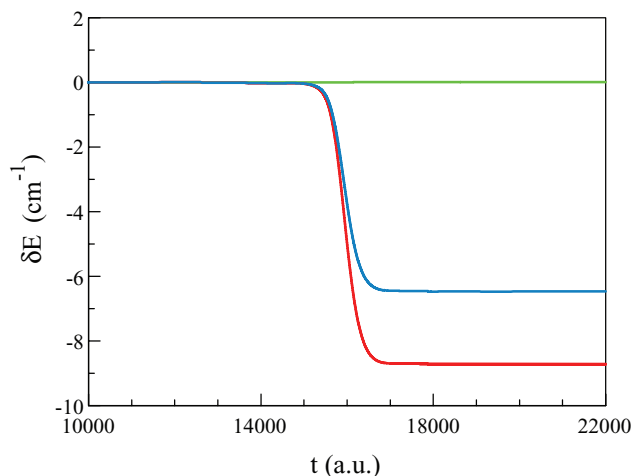


FIG. 6. Total energy conservation in the mixed quantum/classical calculations. Correct method (green) uses Eq. (10') for the mean tensor of inertia. Alternative methods discussed in the text (blue and red) give wrong results, $\delta E \neq 0$.

8.7 cm^{-1} , respectively. Figure 6 shows that energy is lost during the short time interval of the molecule-quencher collision, when response of the molecule to the torque of the quencher is essential. We also checked probabilities of state-to-state transitions in the two test-cases and found that they changed by $\sim 5\%$ and $\sim 10\%$, respectively. This demonstrates that in dynamics calculations one should use only the correct expression for \tilde{I} , that of Eq. (10').

V. CONCLUSIONS

In this paper, we reviewed theory of two mixed quantum/classical approaches to collisional energy transfer and rovibrational energy flow: the heuristic fluid-rotor method (introduced earlier to treat recombination reactions¹¹) and the more rigorous method based on the Ehrenfest theorem.⁴⁷ For the case of diatomic molecule + quencher, we showed analytically that these two methods are entirely equivalent. Notably, they both make use of the average moment of inertia expressed as $\tilde{I} = \langle \Psi(R) | I^{-1}(R) | \Psi(R) \rangle^{-1}$. Although diatomic molecule is the simplest case, this work serves as a proof-of-principle and gives us transparent tools for similar treatments of triatomic and small polyatomic molecules.

Despite the equivalence discussed above, each of the two formulations has its own advantages, and is interesting on its own. For example, the Hamiltonian equations (28a)–(28d) for the diatomic molecule are easier to propagate numerically compared to the fluid-rotor equation (14'). But the fluid-rotor approach gives some additional insight, not immediately present in the Hamiltonian equations of motion (28a)–(28d). One example is the equivalence of the expectation value of quantum rotational potential, Eq. (8), and the classical rotational energy, Eq. (9), which is built into the fluid-rotor

approach and leads to the central equation (10). Second example is the role played by the angular momentum and the torque in Eq. (11). These intuitive features provide better understanding of the mixed quantum/classical methodology. Another important aspect is generality of the fluid-rotor approach. Namely, Eqs. (10), (14), and (17) are expressed in Cartesian coordinates and can be directly applied to basically any molecule (triatomic, small polyatomic), irrespective to the choice of the internal vibrational coordinates.

Numerical results presented here illustrate energy and momentum conservation in the mixed quantum/classical approach and open opportunities for computationally affordable treatment of collisional energy transfer. Calculations of converged cross sections for CO ($v = 1$) quenching by He impact in a broad range of temperatures, $30 < T < 3000 \text{ K}$, are in progress and will be reported in Ref. 50.

ACKNOWLEDGMENTS

Mikhail V. Ivanov at Marquette University is gratefully acknowledged for fruitful discussions. This research was supported by the National Science Foundation (NSF) Atmospheric Chemistry Program, Division of Atmospheric Sciences, Grant No. 0842530. This research used resources of the National Energy Research Scientific Computing Center, which is supported by the Office of Science of the (U.S.) Department of Energy (DOE) under Contract No. DE-AC02-05CH11231.

APPENDIX A: MATRIX EVOLUTION

Substitution of Eqs. (13'), (20), and (21) into Eq. (14') gives

$$\begin{aligned} & \tilde{I} \begin{pmatrix} \sin^2 \gamma \sin^2 \alpha + \cos^2 \gamma & -\sin^2 \gamma \sin \alpha \cos \alpha & -\sin \gamma \cos \gamma \cos \alpha \\ -\sin^2 \gamma \sin \alpha \cos \alpha & \sin^2 \gamma \cos^2 \alpha + \cos^2 \gamma & -\sin \gamma \cos \gamma \sin \alpha \\ -\sin \gamma \cos \gamma \cos \alpha & -\sin \gamma \cos \gamma \sin \alpha & \sin^2 \gamma \end{pmatrix} \begin{pmatrix} 0 & \cos \alpha & \sin \alpha \\ 0 & \sin \alpha & -\cos \alpha \\ 1 & 0 & 0 \end{pmatrix} \begin{pmatrix} \ddot{\alpha} \\ 0 \\ \dot{\gamma} \end{pmatrix} \\ & = \begin{pmatrix} \tau_x \\ \tau_y \\ \tau_z \end{pmatrix} - \begin{pmatrix} \sin^2 \gamma \sin^2 \alpha + \cos^2 \gamma & -\sin^2 \gamma \sin \alpha \cos \alpha & -\sin \gamma \cos \gamma \cos \alpha \\ -\sin^2 \gamma \sin \alpha \cos \alpha & \sin^2 \gamma \cos^2 \alpha + \cos^2 \gamma & -\sin \gamma \cos \gamma \sin \alpha \\ -\sin \gamma \cos \gamma \cos \alpha & -\sin \gamma \cos \gamma \sin \alpha & \sin^2 \gamma \end{pmatrix} \\ & \times \left(\tilde{I} \begin{pmatrix} 0 & \cos \alpha & \sin \alpha \\ 0 & \sin \alpha & -\cos \alpha \\ 1 & 0 & 0 \end{pmatrix} + \tilde{I} \dot{\alpha} \begin{pmatrix} 0 & -\sin \alpha & \cos \alpha \\ 0 & \cos \alpha & \sin \alpha \\ 0 & 0 & 0 \end{pmatrix} \right) \begin{pmatrix} \dot{\alpha} \\ 0 \\ \dot{\gamma} \end{pmatrix} \\ & - \tilde{I} \dot{\gamma} \begin{pmatrix} \sin 2\gamma \sin^2 \alpha - \sin 2\gamma & -\sin 2\gamma \sin \alpha \cos \alpha & -\cos 2\gamma \cos \alpha \\ -\sin 2\gamma \sin \alpha \cos \alpha & \sin 2\gamma \cos^2 \alpha - \sin 2\gamma & -\cos 2\gamma \sin \alpha \\ -\cos 2\gamma \cos \alpha & -\cos 2\gamma \sin \alpha & 2 \sin \gamma \cos \gamma \end{pmatrix} \begin{pmatrix} 0 & \cos \alpha & \sin \alpha \\ 0 & \sin \alpha & -\cos \alpha \\ 1 & 0 & 0 \end{pmatrix} \begin{pmatrix} \dot{\alpha} \\ 0 \\ \dot{\gamma} \end{pmatrix} \\ & - \tilde{I} \dot{\alpha} \begin{pmatrix} \sin^2 \gamma \sin 2\alpha & -\sin^2 \gamma \cos 2\alpha & \sin \gamma \cos \gamma \sin \alpha \\ -\sin^2 \gamma \cos 2\alpha & -\sin^2 \gamma \sin 2\alpha & -\sin \gamma \cos \gamma \cos \alpha \\ \sin \gamma \cos \gamma \sin \alpha & -\sin \gamma \cos \gamma \cos \alpha & 0 \end{pmatrix} \begin{pmatrix} 0 & \cos \alpha & \sin \alpha \\ 0 & \sin \alpha & -\cos \alpha \\ 1 & 0 & 0 \end{pmatrix} \begin{pmatrix} \dot{\alpha} \\ 0 \\ \dot{\gamma} \end{pmatrix}. \end{aligned}$$

Three components of this matrix equation can be analyzed separately. For x -component, we obtain

$$\begin{aligned} \tilde{I}(\dot{\gamma} \sin \alpha - \ddot{\alpha} \sin \gamma \cos \gamma \cos \alpha) &= \tilde{\tau}_x - \dot{\tilde{I}}(\dot{\gamma} \sin \alpha - \dot{\alpha} \sin \gamma \cos \gamma \cos \alpha) \\ &\quad - \tilde{I} \dot{\alpha} \dot{\gamma} \cos^2 \gamma \cos \alpha + \tilde{I} \dot{\alpha} \dot{\gamma} \cos 2\gamma \cos \alpha + \tilde{I} \dot{\alpha} \dot{\gamma} \sin^2 \gamma \cos \alpha - \tilde{I} \dot{\alpha}^2 \sin \gamma \cos \gamma \sin \alpha \\ &= \tilde{\tau}_x - \dot{\tilde{I}}(\dot{\gamma} \sin \alpha - \dot{\alpha} \sin \gamma \cos \gamma \cos \alpha) - \tilde{I} \dot{\alpha}^2 \sin \gamma \cos \gamma \sin \alpha. \end{aligned} \quad (\text{A1})$$

For y -component, we obtain

$$\begin{aligned} \tilde{I}(-\dot{\gamma} \cos \alpha - \ddot{\alpha} \sin \gamma \cos \gamma \sin \alpha) &= \tilde{\tau}_y - \dot{\tilde{I}}(-\dot{\gamma} \cos \alpha - \dot{\alpha} \sin \gamma \cos \gamma \sin \alpha) \\ &\quad - \tilde{I} \dot{\alpha} \dot{\gamma} \cos^2 \gamma \sin \alpha + \tilde{I} \dot{\alpha} \dot{\gamma} \cos 2\gamma \sin \alpha + \tilde{I} \dot{\alpha} \dot{\gamma} \sin^2 \gamma \sin \alpha + \tilde{I} \dot{\alpha}^2 \sin \gamma \cos \gamma \cos \alpha \\ &= \tilde{\tau}_y - \dot{\tilde{I}}(-\dot{\gamma} \cos \alpha - \dot{\alpha} \sin \gamma \cos \gamma \sin \alpha) + \tilde{I} \dot{\alpha}^2 \sin \gamma \cos \gamma \cos \alpha. \end{aligned} \quad (\text{A2})$$

For z -component, we obtain

$$\begin{aligned} \tilde{I} \ddot{\alpha} \sin^2 \gamma &= \tilde{\tau}_z - (\dot{\tilde{I}} \dot{\alpha} \sin^2 \gamma + \tilde{I} \dot{\gamma} \dot{\alpha} \sin \gamma \cos \gamma + 2\tilde{I} \dot{\gamma} \dot{\alpha} \sin \gamma \cos \gamma - \tilde{I} \dot{\gamma} \dot{\alpha} \sin \gamma \cos \gamma) \\ &= \tilde{\tau}_z - \dot{\tilde{I}} \dot{\alpha} \sin^2 \gamma - 2\tilde{I} \dot{\gamma} \dot{\alpha} \sin \gamma \cos \gamma. \end{aligned} \quad (\text{A3})$$

APPENDIX B: CHAIN RULE

Although in Sec. III A we expressed \tilde{V} as a function of $\mathbf{R}_C = \{\mathbf{q}_{\text{mol}}, \mathbf{q}_{\text{que}}, \alpha, \gamma\}$, here we will have to switch variables to Cartesian coordinates with respect to molecular center of mass, $\mathbf{r}_1 = \{x_1, y_1, z_1\}$ and $\mathbf{r}_2 = \{x_2, y_2, z_2\}$, defined by Eqs. (18a)–(18c) and consistent with Eq. (17). Using the chain rule of differentiation, we can write

$$\begin{aligned} \frac{\partial \tilde{V}}{\partial \alpha} &= \frac{\partial \tilde{V}}{\partial x_1} \frac{\partial x_1}{\partial \alpha} + \frac{\partial \tilde{V}}{\partial x_2} \frac{\partial x_2}{\partial \alpha} + \frac{\partial \tilde{V}}{\partial y_1} \frac{\partial y_1}{\partial \alpha} \\ &\quad + \frac{\partial \tilde{V}}{\partial y_2} \frac{\partial y_2}{\partial \alpha} + \frac{\partial \tilde{V}}{\partial z_1} \frac{\partial z_1}{\partial \alpha} + \frac{\partial \tilde{V}}{\partial z_2} \frac{\partial z_2}{\partial \alpha} \\ &= -\frac{\partial \tilde{V}}{\partial x_1} y_1 - \frac{\partial \tilde{V}}{\partial x_2} y_2 + \frac{\partial \tilde{V}}{\partial y_1} x_1 + \frac{\partial \tilde{V}}{\partial y_2} x_2. \end{aligned} \quad (\text{B1})$$

Here, we used the following properties: $\partial x_i / \partial \alpha = -y_i$, $\partial y_i / \partial \alpha = x_i$, and $\partial z_i / \partial \alpha = 0$, which follow from the definitions of Eqs. (18a)–(18c). Introducing forces expressed in Cartesian coordinates, rearranging the terms, and using the definition of torque $\boldsymbol{\tau} = \mathbf{r} \times \mathbf{F}$, we obtain

$$\begin{aligned} \frac{\partial \tilde{V}}{\partial \alpha} &= \tilde{F}_{x_1} y_1 - \tilde{F}_{y_1} x_1 + \tilde{F}_{x_2} y_2 - \tilde{F}_{y_2} x_2 \\ &= -\tilde{\tau}_{z_1} - \tilde{\tau}_{z_2} = -\sum_i \tilde{\tau}_{z_i} = -\tilde{\tau}_z. \end{aligned} \quad (\text{B2})$$

Here, summation is over two atoms in the diatomic, just as in Eq. (17).

Similarly, using Eqs. (18a)–(18c) we can write

$$\begin{aligned} \frac{\partial \tilde{V}}{\partial \gamma} &= \frac{\partial \tilde{V}}{\partial x_1} \frac{\partial x_1}{\partial \gamma} + \frac{\partial \tilde{V}}{\partial x_2} \frac{\partial x_2}{\partial \gamma} + \frac{\partial \tilde{V}}{\partial y_1} \frac{\partial y_1}{\partial \gamma} + \frac{\partial \tilde{V}}{\partial y_2} \frac{\partial y_2}{\partial \gamma} \\ &\quad + \frac{\partial \tilde{V}}{\partial z_1} \frac{\partial z_1}{\partial \gamma} + \frac{\partial \tilde{V}}{\partial z_2} \frac{\partial z_2}{\partial \gamma} \end{aligned}$$

$$\begin{aligned} &= \frac{\partial \tilde{V}}{\partial x_1} z_1 \cos \alpha + \frac{\partial \tilde{V}}{\partial x_2} z_2 \cos \alpha + \frac{\partial \tilde{V}}{\partial y_1} z_1 \sin \alpha \\ &\quad + \frac{\partial \tilde{V}}{\partial y_2} z_2 \sin \alpha - \frac{\partial \tilde{V}}{\partial z_1} (x_1 \cos \alpha + y_1 \sin \alpha) \\ &\quad - \frac{\partial \tilde{V}}{\partial z_2} (x_2 \cos \alpha + y_2 \sin \alpha). \end{aligned} \quad (\text{B3})$$

Introducing forces expressed in Cartesian coordinates, rearranging the terms and using the definition of torque, we obtain

$$\begin{aligned} \frac{\partial \tilde{V}}{\partial \gamma} &= (\tilde{F}_{z_1} x_1 - \tilde{F}_{x_1} z_1 + \tilde{F}_{z_2} x_2 - \tilde{F}_{x_2} z_2) \cos \alpha \\ &\quad + (\tilde{F}_{z_1} y_1 - \tilde{F}_{y_1} z_1 + \tilde{F}_{z_2} y_2 - \tilde{F}_{y_2} z_2) \sin \alpha \\ &= \sum_i \tilde{\tau}_{y_i} \cos \alpha - \sum_i \tilde{\tau}_{x_i} \sin \alpha \\ &= \tilde{\tau}_y \cos \alpha - \tilde{\tau}_x \sin \alpha. \end{aligned} \quad (\text{B4})$$

¹V. Bernshtein and I. Oref, *Isr. J. Chem.* **47**, 205 (2008).

²M.-L. Dubernet, F. Daniel, A. Grosjean, and C. Y. Lin, *Astron. Astrophys.* **497**, 911 (2009).

³F. Daniel, M.-L. Dubernet, F. Pacaud, and A. Grosjean, *Astron. Astrophys.* **517**, A13 (2010).

⁴F. Daniel, M.-L. Dubernet, and A. Grosjean, *Astron. Astrophys.* **536**, A76 (2011).

⁵L. Wiesenfeld, Y. Scribano, and A. Faure, *Phys. Chem. Chem. Phys.* **13**, 8230 (2011).

⁶C. H. Yang, G. Sarma, D. H. Parker, J. J. ter Meulen, and L. Wiesenfeld, *J. Chem. Phys.* **134**, 204308 (2011).

⁷N. Balakrishnan, A. Dalgarno, and R. C. Forrey, *J. Chem. Phys.* **113**, 621 (2000).

⁸C. Cecchi-Pestellini, E. Bodo, N. Balakrishnan, and A. Dalgarno, *Astro-phys. J.* **571**, 1015 (2002).

⁹B. Kendrick and R. Pack, *Chem. Phys. Lett.* **235**, 291 (1995).

¹⁰R. T. Pack, R. B. Walker, and B. K. Kendrick, *J. Chem. Phys.* **109**, 6701 (1998).

¹¹M. Ivanov and D. Babikov, *J. Chem. Phys.* **134**, 144107 (2011).

¹²M. Ivanov and D. Babikov, *J. Chem. Phys.* **134**, 174308 (2011).

¹³M. Ivanov and D. Babikov, *J. Chem. Phys.* **136**, 184304 (2012).

- ¹⁴M. Tacconi and F. A. Gianturco, *J. Chem. Phys.* **131**, 094301 (2009).
- ¹⁵N. Balakrishnan, G. Quéméner, R. C. Forrey, R. J. Hinde, and P. C. Stancil, *J. Chem. Phys.* **134**, 014301 (2011).
- ¹⁶L. M. C. Janssen, P. S. Zuchowsky, A. van der Avoird, J. M. Hudson, and G. C. Groenenboom, *J. Chem. Phys.* **134**, 124309 (2011).
- ¹⁷G. Quéméner, N. Balakrishnan, and B. K. Kendrick, *J. Chem. Phys.* **129**, 224309 (2008).
- ¹⁸G. A. Parker, R. B. Walker, B. K. Kendrick, and R. T Pack, *J. Chem. Phys.* **117**, 6083 (2002).
- ¹⁹D. K. Havey, Q. Liu, Z. Li, M. Elioff, and A. S. Mullin, *J. Phys. Chem. A* **111**, 13321 (2007).
- ²⁰D. K. Havey, J. Du, and A. S. Mullin, *J. Phys. Chem. A* **114**, 1569 (2010).
- ²¹T. D. Sechler, L. P. Dempsey, and M. I. Lester, *J. Phys. Chem. A* **113**, 8845 (2009).
- ²²L. P. Dempsey, T. D. Sechler, C. Murray, and M. I. Lester, *J. Phys. Chem. A* **113**, 6851 (2009).
- ²³A. L. Brunsfold, D. J. Garton, T. K. Minton, D. Troya, and G. C. Schatz, *J. Chem. Phys.* **121**, 11702 (2004).
- ²⁴C.-L. Liu, H. C. Hsu, J.-J. Lyu, and C.-K. Ni, *J. Chem. Phys.* **123**, 131102 (2005).
- ²⁵R. X. Fernandes, K. Luther, J. Troe, and V. G. Ushakov, *Phys. Chem. Chem. Phys.* **10**, 4313 (2008).
- ²⁶V. Bernshtein and I. Oref, *J. Chem. Phys.* **125**, 133105 (2006).
- ²⁷A. W. Jasper and J. A. Miller, *J. Phys. Chem. A* **113**, 5612 (2009).
- ²⁸J. R. Barker, *Int. J. Chem. Kinet.* **41**, 748 (2009).
- ²⁹D. M. Golden and J. R. Barker, *Combust. Flame* **158**, 602 (2011).
- ³⁰A. L. Kaledin, X. Huang, and J. M. Bowman, *Chem. Phys. Lett.* **384**, 80 (2004).
- ³¹G. Czakó, A. L. Kaledin, and J. M. Bowman, *J. Chem. Phys.* **132**, 164103 (2010).
- ³²G. D. Billing, *Comput. Phys. Rep.* **1**, 239 (1984).
- ³³G. S. Whittier and J. C. Light, *J. Chem. Phys.* **110**, 4280 (1999).
- ³⁴D. Babikov, F. Aguillon, M. Sizun, and V. Sidis, *Phys. Rev. A* **59**, 330 (1999).
- ³⁵M. Sizun, F. Aguillon, V. Sidis, V. Zenevich, G. D. Billing, and N. Markovi, *Chem. Phys.* **209**, 327 (1996).
- ³⁶F. Aguillon, V. Sidis, and J. P. Gauyacq, *J. Chem. Phys.* **95**, 1020 (1991).
- ³⁷M. Sizun and F. Aguillon, *Chem. Phys.* **226**, 47 (1998).
- ³⁸M. Ivanov and D. Babikov, "On molecular origin of mass-independent fractionation of oxygen isotopes in the ozone forming recombination reaction," *Proc. Natl. Acad. Sci. U.S.A.* (published online).
- ³⁹T. J. Park and J. C. Light, *J. Chem. Phys.* **85**, 5870 (1986).
- ⁴⁰H. Goldstein, *Classical Mechanics* (Addison-Wesley, Reading, MA, 1965).
- ⁴¹J. M. Bowman, *Chem. Phys. Lett.* **217**, 36 (1994).
- ⁴²J. Qi and J. M. Bowman, *J. Chem. Phys.* **105**, 9884 (1996).
- ⁴³J. Qi and J. M. Bowman, *J. Chem. Phys.* **107**, 9960 (1997).
- ⁴⁴S. Carter and J. M. Bowman, *J. Chem. Phys.* **108**, 4397 (1998).
- ⁴⁵S. Skokov and J. Bowman, *J. Chem. Phys.* **110**, 9789 (1999).
- ⁴⁶S. Zou, S. Skokov, and J. M. Bowman, *J. Phys. Chem. A* **105**, 2423 (2001).
- ⁴⁷D. J. Tannor, *Introduction to Quantum Mechanics: A Time-dependent Perspective* (University Science Books, 2007).
- ⁴⁸J. C. Tully, *J. Chem. Phys.* **93**, 1061 (1990).
- ⁴⁹B. Podolsky, *Phys. Rev.* **32**, 812 (1928).
- ⁵⁰A. Semenov, M. Ivanov, and D. Babikov, "Ro-vibrational quenching of CO($v=1$) by He impact in a broad range of temperatures: A benchmark study using mixed quantum/classical inelastic scattering theory" (unpublished).
- ⁵¹W. H. Press, B. P. Flannery, S. A. Teukolsky, and W. T. Vetterling, *Numerical Recipes* (Cambridge University Press, 1989).